© 2022. Published by The Company of Biologists Ltd | Journal of Experimental Biology (2022) 225, jeb243917. doi:10.1242/jeb.243917

RESEARCH ARTICLE

Echolocating Daubenton's bats call louder, but show no spectral jamming avoidance in response to bands of masking noise during a landing task

Michael Bjerre Pedersen*, Astrid Særmark Uebel, Kristian Beedholm, Ilias Foskolos, Laura Stidsholt and Peter Teglberg Madsen

ABSTRACT

Echolocating bats listen for weak echoes to navigate and hunt, which makes them prone to masking from background noise and jamming from other bats and prey. As for electrical fish that display clear spectral jamming avoidance responses (JAR), bats have been reported to mitigate the effects of jamming by shifting the spectral contents of their calls, thereby reducing acoustic interference to improve echo-to-noise ratio (ENR). Here, we tested the hypothesis that frequency-modulating bats (FM bats) employ a spectral JAR in response to six masking noise bands ranging from 15 to 90 kHz, by measuring the −3 dB endpoints and peak frequency of echolocation calls from five male Daubenton's bats (*Myotis daubentonii*) during a landing task. The bats were trained to land on a noise-generating spherical transducer surrounded by a star-shaped microphone array, allowing for acoustic localization and source parameter quantification of on-axis calls. We show that the bats did not employ spectral JAR as the peak frequency during jamming remained unaltered compared with that of silent controls (all $P>0.05$, 60.73±0.96 kHz, mean±s.e.m.), and −3 dB endpoints decreased in noise irrespective of treatment type. Instead, Daubenton's bats responded to acoustic jamming by increasing call amplitude via a Lombard response that was bandwidth dependent, ranging from a mean of 0.05 dB/dB (95% confidence interval 0.04–0.06 dB/dB) noise for the most narrowband noise (15–30 kHz) to 0.17 dB/dB (0.16–0.18 dB/dB) noise for the most broadband noise (30–90 kHz). We conclude that Daubenton's bats, despite having the vocal flexibility to do so, do not employ a spectral JAR, but defend ENRs via a bandwidth-dependent Lombard response.

KEY WORDS: Chiroptera, Biosonar, Jamming avoidance response, Lombard response, Acoustic interference

INTRODUCTION

Bats navigate and hunt under light-limited conditions using an acute biosonar system (Griffin, 1958). By actively emitting powerful, directional calls at ultrasonic frequencies, echolocating bats generate echoes from their environment for auditory processing to inform changes in motor patterns (Griffin and Galambos, 1940, 1941). Successful detection and processing of returning weak prey echoes is critical for their foraging success and depends on the outgoing source level (SL); the two-way transmission loss to the target of interest and back (TL); and the target strength (TS) of the ensonified target and the detection threshold of the receiving auditory system (Au, 1993; Møhl, 1988). Noise with spectral, temporal and spatial overlap will mask the returning echoes by raising the detection threshold, if the noise exceeds the hearing threshold of the receiver. Sources of such masking noise may be physical (e.g. wind, rain), anthropogenic (e.g. traffic noise) or stem from other animals (e.g. bats and insect). When acoustic signals from other bats or prey inadvertently or deliberately reduce the biosonar performance through interference, it is coined acoustic jamming (Jones et al., 2021). Some bat species live in roosts composed of thousands to millions of individuals where they are probably subjected to intense jamming by echolocating conspecifics, and indeed laboratory playback studies suggest that jamming from bat calls directly reduces capture success of insect targets (Corcoran and Conner, 2014).

One way to ameliorate the effects of jamming is the 'jamming avoidance response' (JAR). It was first discovered in weakly electric fishes which shift discharge frequency in response to both electrical stimuli and nearby conspecifics (Bullock et al., 1972; Scheich, 1977). Inspired by this work, bat researchers began to investigate whether bats similarly mitigate the effects of jamming by spectrally shifting their echolocation calls in response to vocalizing conspecifics to maintain echo-to-noise ratio (ENR) sufficient for detection and processing.

The earliest work on biosonar performance in bats by Griffin et al. (1963) demonstrated that bats have remarkable resilience to masking noise during a wire avoidance task (with reduced performance at higher noise bandwidths), but the study did not address whether the bats exhibited any spectral JAR in response to masking noise. Since the pioneering work of Griffin et al. (1963), a wealth of more recent studies on both wild and captive bats report that bats exhibit a spectral JAR when flying with conspecifics (Chiu et al., 2009; Habersetzer, 1981; Ibáñez et al., 2004; Obrist, 1995; Ratcliffe et al., 2004; Surlykke and Moss, 2000; Ulanovsky et al., 2004) and heterospecifics (Necknig and Zahn, 2011), and in response to artificial playback noise (Bates et al., 2008; Gillam and Montero, 2016; Gillam et al., 2007; Tressler and Smotherman, 2009). The overall magnitude of the spectral response reported in these studies varies from 0.5 to 8 kHz measured as peak, maximum and minimum frequency. Such spectral changes may indeed be a result of JAR but, without knowledge about the range to the bat and the pointing axis of its directional beam in relation to the recording microphone, the low-pass filtering effects of frequency-specific absorption and off-axis distortion on the recorded calls (Au et al., 2012; Smith et al., 2019) could lead to similar spectral shifts in the

Marine Bioacoustics Lab, Zoophysiology, Department of Biology, Aarhus University, 8000 Aarhus, Denmark.

*Author for correspondence (michael.pedersen@bio.au.dk)

M.B.P., 0000-0002-6215-5097; K.B., 0000-0001-5699-0849; I.F., 0000-0003-1951-9382; L.S., 0000-0002-2187-7835; P.T.M., 0000-0002-5208-5259

Received 17 December 2021; Accepted 2 March 2022

absence of any JAR. More recent work has used acoustic tags, which offer a recording aspect with consistent spectral distortion, and/or microphone arrays with a sufficient number of receivers to allow for acoustic localization and direction of beam pointing. These studies have provided more mixed results, with some showing a spectral JAR (Luo and Moss, 2017; Takahashi et al., 2014) and others not (Amichai et al., 2015; Cvikel et al., 2015; Götze et al., 2016). Rather than a decrease in spectral overlap, bats may instead defend ENRs by increasing call intensity (Amichai et al., 2015; Cvikel et al., 2015; Foskolos et al., 2022; Lu et al., 2020; Luo et al., 2016) in the form of a Lombard response (Lombard, 1911).

It is thus known (i) that the difficulty of a wire avoidance task increases with total noise bandwidth (Griffin et al., 1963), (ii) that bats can elicit a Lombard response when exposed to masking noise (Foskolos et al., 2022; Lu et al., 2020; Luo et al., 2016) or conspecific calls (Amichai et al., 2015), and (iii) that evidence for a spectral JAR in echolocating bats is inconsistent. To understand whether JAR plays a significant role in the response of the bat biosonar system to noise, it is critical to quantify whether and how echolocating bats spectrally respond to a well-defined task under masking conditions with on-axis quantification of spectral call parameters. In this study, we sought to meet these requirements by training Daubenton's bats [*Myotis daubentonii* (Kuhl 1817)] to land on a spherical target that could also transmit six different types of band-limited noise at the same intensity, either just outside or overlapping to different degrees the frequency range of the first harmonic of their approach calls. We chose Daubenton's bats because they can shift the peak frequency of their echolocation calls by almost an octave as they transition from the approach to the buzz phase (Fig. 1), thereby displaying the vocal plasticity needed to employ an effective JAR under the experimental scheme used here. We hypothesized that if a spectral JAR is exhibited by the bats, low-frequency noise should elicit an increase in peak frequency and high-frequency noise in turn should elicit a decrease in peak frequency. Conversely, if a spectral JAR is not used to improve ENRs, we hypothesized that the studied bats would instead increase call amplitude (Lombard response) in response to broadband masking noise. We show that when Daubenton's bats are faced with bands of masking noise, they perform no spectral JAR, but instead exhibit a Lombard response by increasing their SLs proportionally to the total bandwidth of the masking noise.

MATERIALS AND METHODS

Animal husbandry and training

We used five wild-caught, adult, male Daubenton's bats of unknown age caught in Hobro, Denmark, with mist nets. The bats were kept on a diet of mealworms (larval form of *Tenebrio molitor*) and supplemented with vitamin-paste (NUTRI-CAL, Tomlyn, Fort Worth, TX, USA). The bats were housed in a temperature- and humidity-controlled roost at Aarhus University on a 12 h:12 h inverted light:dark schedule. The mass of all five bats was maintained between 7 and 9 g. Using operant conditioning, all bats were trained in a dark (<<0.01 lx) anechoic room to land on a transducer (HS-26, Sonar products, Driffield, UK; measured target strength of −15 dB at 0.1 m) that could emit noise and was protruding from a microphone array covered in anechoic foam (Fig. 2). The bats were trained both when the target was silent and when it was transmitting one of six calibrated noise signals of varying bandwidth. Correct behavior (e.g. landing) was rewarded with a mealworm, and incorrect behavior involved a short time-out of ∼30 s and no food reward. Bats were trained for approximately 4 weeks to land on the target. Training was complete when they could consistently perform the task at the highest noise levels. Capture in the wild was made under permit MST-850-00064 and all experiments were performed under permit 2016-15-0201-00989 issued by The Animal Experimentation Inspectorate under The Ministry of Environment and Food of Denmark to Prof. Peter T. Madsen. The bats were released back into the wild at the capture site at the end of the experimental period.

Experimental design

Sessions were conducted in the morning from 09:00 h to 12:00 h. All trials were performed in the 5×4×2.5 m anechoic testing chamber at Zoophysiology, Aarhus University, Denmark.

The room was lined with acoustic foam, which is anechoic at ultrasonic frequencies (measured reflectivity of −30 dB re. hard wall from 10 to 100 kHz). The same foam covered a custom-built star-shaped array with seven calibrated Knowles microphones (FG-3329, Knowles Electronics, Itasca, IL, USA). The array had a maximum horizontal aperture of 1.2 m, allowing for accurate acoustic localizations at distances of 6–12 m (5–10 times aperture) (Kyhn et al., 2009; Macaulay et al., 2017; Stidsholt et al., 2020). One microphone was placed immediately below the target transducer for on-axis quantification of calls. Calibration sweeps played from an ultrasonic loudspeaker (Vifa, part #60108, Avisoft Bioacoustics, Glienicke/Nordbahn, Germany) at known coordinates with respect to the array resulted in differences between measured and calculated transmission losses of <2 dB. The Knowles microphone signals were amplified by a custom-built filtering and gain box (1 pole, 1 kHz high-pass filter, 4 pole, 100 kHz anti-aliasing filter, 30 dB gain; Aarhus University Electronics workshop). All microphones were digitized in a multi-channel analog-to-digital converter (USB-6356, National Instruments, Houston, TX, USA) sampling at 400 kHz per channel, 16 bit.

The target transducer was connected to a battery powered amplifier (Marchand BE01 Piezo Transducer Amplifier) and transmitted calibrated flat (±2 dB) broadband noise at 1 m distance in the following frequency bands (kHz): 15–30, 30–45, 30–55, 30–90, 55–90 and 70–90 (Fig. 3). Two bandwidths which spanned the lower (30–45, 30–55 kHz treatments) and higher (55–90, 70–90 kHz) were chosen to vary the ease with which a spectral JAR would serve to uphold ENRs. The 15–30 kHz and 30–90 kHz noise-bands were included as negative controls for an out-of-band noise induced Lombard response and a Lombard response when spectral shifts were not possible, respectively. The noise was equalized by correcting for the transfer function of the HS-26 transducer as measured at 1 m distance. Daubenton's bats exhibit a clear Lombard response at broadband noise levels exceeding 74 dB re. 20 µPa root mean square (RMS) at 1 m (Foskolos et al., 2022). We therefore calibrated all noise bands to a broad band SL of 72 dB re. 20 µPa RMS using a G.R.A.S. microphone (46DP 1/8 inch, GRAS Sound & Vibration, Holte, Denmark, www.gras.dk; sensitivity 156 dB re. 20 µPa V^{-1}). This level was a compromise between achieving as prominent a Lombard response as possible and the highest noise level achievable for the noise bands in the frequency range where the transducer was least sensitive (70–90 kHz). Data acquisition and noise playback controls were performed with a custom-written program (using Labview v.2015f, National Instruments). Every morning, the noise playback of each noise band was tested to ensure consistency in noise levels over time, and the array microphones were calibrated before and after completion of all trials.

Journal of Experimental Biology (2022) 225, jeb243917. doi:10.1242/jeb.243917

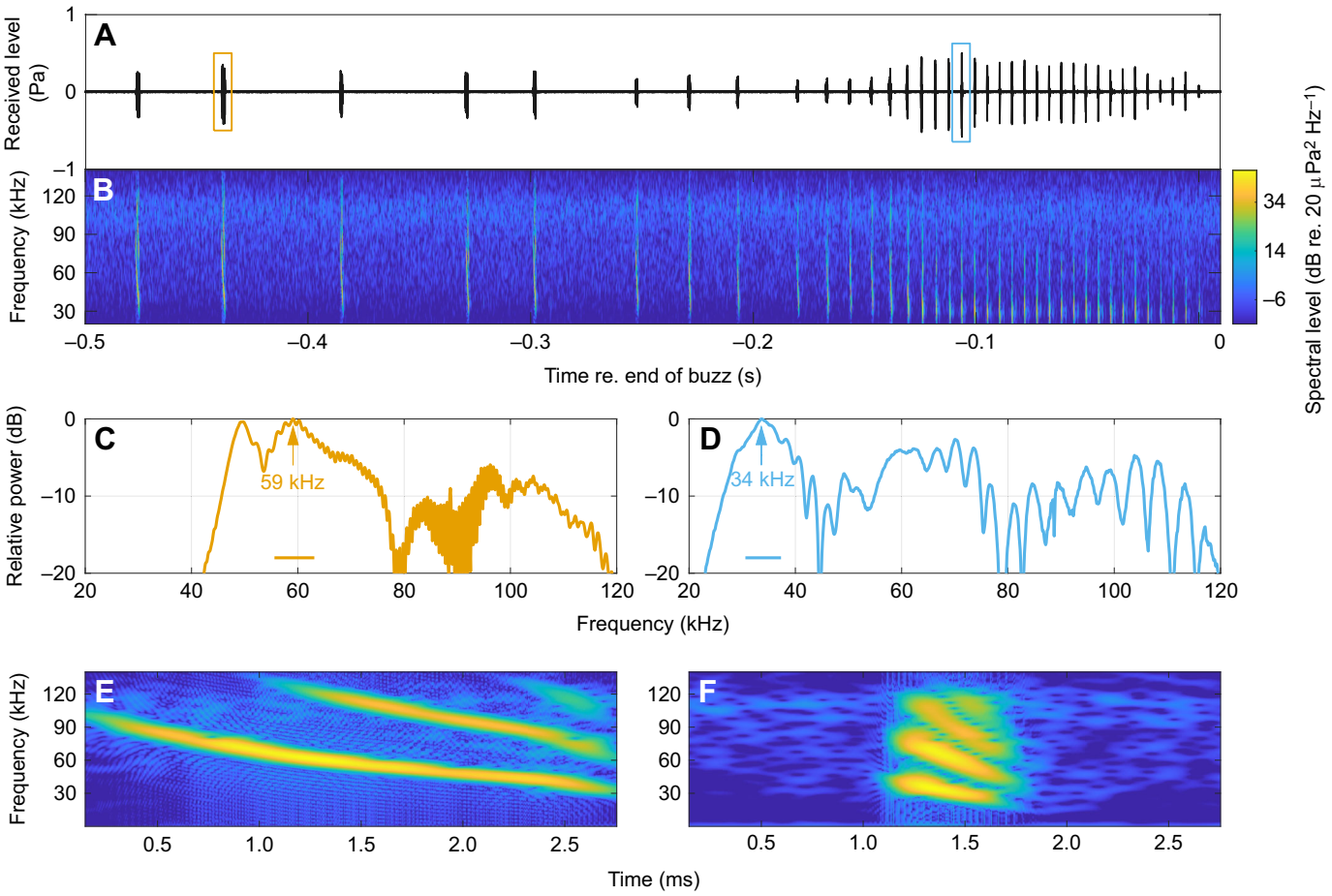

Fig. 1. Example target approach of a Daubenton's bat. (A) Time series of a control trial for one of the bats with an approach and buzz phase before landing. (B) Spectrogram of the same trial. (C) Relative power spectrum of an approach call. Horizontal line denotes the half-power bandwidth (55.6–63.1 kHz). (D) Relative power spectrum of a buzz call. Horizontal line denotes the half-power bandwidth (30.6–37.3 kHz). (E) Spectrogram of an approach call. (F) Spectrogram of a buzz call. Peak frequency changes from ∼59 kHz during approach calls (C: peak frequency denoted by arrow, orange box in A) to ∼34 kHz for buzz calls (D: peak frequency denoted by arrow, blue box in A). Spectrogram settings: sampling rate 400 kHz, FFT chunk 128 points, 97.5% overlap, Hann window, FFT size 1024 points (zero padding); frequency resolution 3.1 kHz; time resolution 8 µs. Power spectrum settings: FFT size: 4000 points, bin width 100 Hz.

The bats were released from the hand of a blinded experimenter 4 m from the target at the start of each trial. A second experimenter controlled the playback and triggered saving of the recording upon successful completion of the landing task monitored by an infrared camera (TV IP310PI, TRENDnet, Torrance, CA, USA). On each experimental day, the bats were exposed to all the noise bands 3 times with blank no-noise trials following each noise exposure for a total of approximately 36 trials per day and bat. If a bat either refused to do the task or lost motivation on any given day, it was put into the holding cage with access to food and water.

Data analysis

Acoustic localization and call selection

The PAMGuard click detector module (v.2.01.03, www.pamguard.org) (Gillespie et al., 2009) was used to detect the onset of the bat calls on each microphone and calculate time delay measurements using cross-correlation between channels. Calls were then manually marked from each trial. For trials where the bat had multiple approach attempts before successfully landing, only the final attempt was stored for future analysis. The call waveforms, and time delay measurements were then imported into MATLAB R2018b (MathWorks, Natick, MA, USA) using the public PAMGuard MATLAB library (www.sourceforge.net/projects/pamguard). We used the time delay measurements of each call to calculate the 3D location with a simplex minimization algorithm (Nelder and Mead, 1965). From the 3D-coordinate, we could then calculate the range to each microphone for subsequent parameter estimation. We selected the five loudest calls from each trial from the microphone immediately below the target transducer as approximate on-axis calls. The microphone below the target transducer had the lowest received noise level of the microphones in the vertical plane of the target, allowing for the smallest interference of noise on parameter quantification. The spectra of all calls recorded this way in no-noise trials were remarkably stereotyped (Fig. S1), the flight paths towards the target did not differ across treatments (Fig. S3), and the same calls on all the surrounding microphones had evident low-pass filtering from off-axis distortion (see below). These points taken together lend credence to the use of this microphone for extraction of on-axis calls.

Quantification of call parameters

Call filtering

Call parameter quantification is sensitive to noise. As the transducer was embedded at the center of the microphone array, all

Journal of Experimental Biology (2022) 225, jeb243917. doi:10.1242/jeb.243917

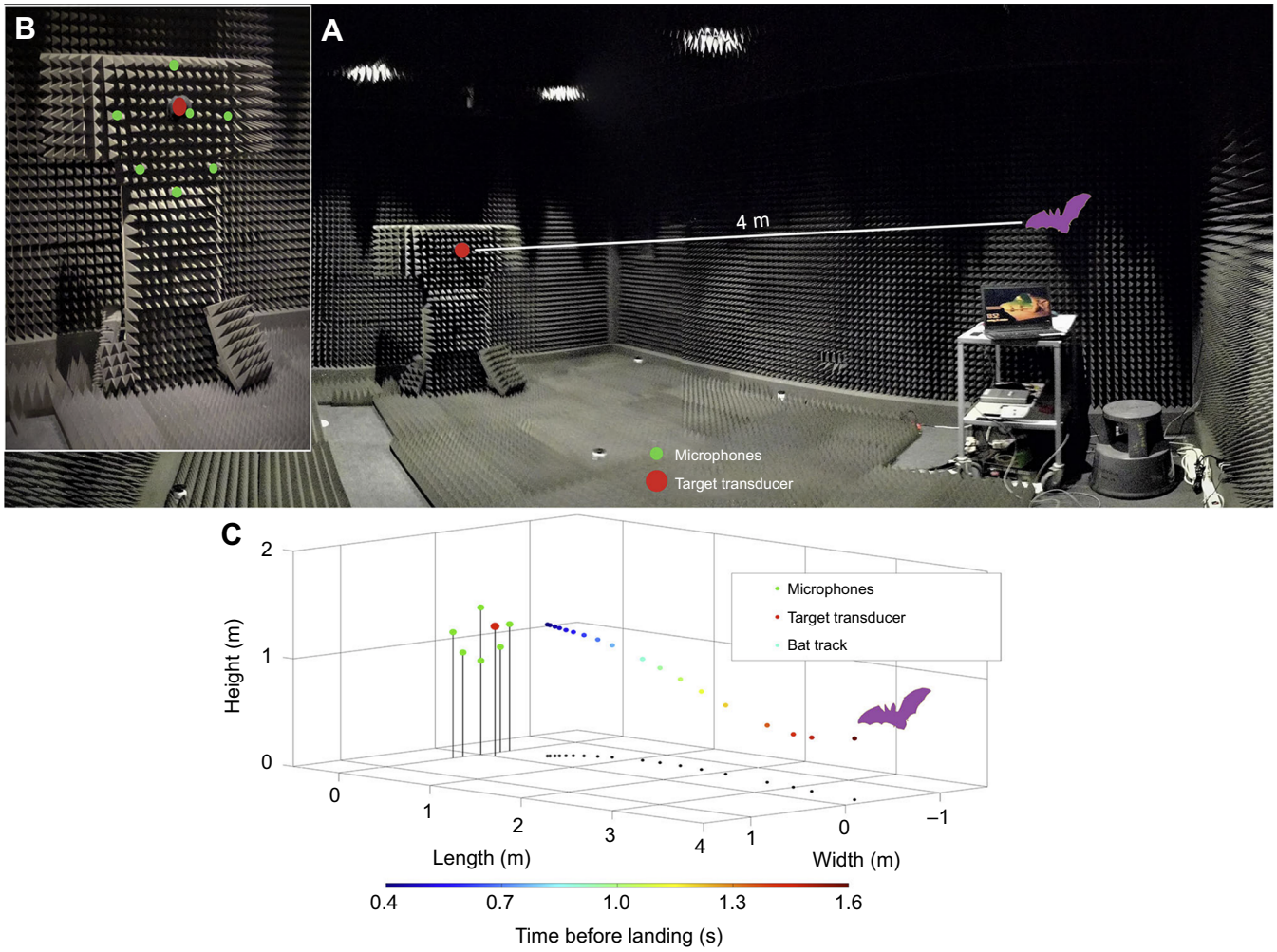

Fig. 2. Overview of the experimental setup. (A) The anechoic room in which experiments were performed. Bats were released in the far end of the room and were trained to approach and land on a target (red circle). Landing was monitored via a laptop from the live feed of a ceiling-mounted infrared camera. (B) Surrounding the transducer is a star-shaped microphone array for acoustic localization. (C) Example track of a bat's flight path when approaching the array. From Foskolos et al. (2022), which used the same setup with a smaller maximum horizontal array aperture (0.8 m vs 1.2 m).

microphones were recording high noise levels. To mitigate this issue, we implemented a fast Fourier transform (FFT) filter to remove noise prior to parameter extraction. We computed the power spectrum of each call with a Tukey window and zero-padding up to the FT window size (4000 points). To remove the noise, we used the first 125 ms of the audio file for each trial to spectrally quantify the noise as received on each microphone in the absence of bat calls. We did this by computing the power spectrum of the noise (FFT size: 4000 points, bin width 100 Hz) and applying a 10-point (1 kHz width) moving average to smooth out the noise, while preserving the original amplitude. We then subtracted the smoothed noise signal from the power spectrum of the bat call signal (in linear units). Remaining peaks in the spectrum with a width of 1 bin (100 Hz) and with neighboring bins of amplitude ≤ 0 were also classified as noise and set to zero. All bins with a value ≤ 0 were set to the minimum positive value of the spectrum to avoid results with complex values in subsequent steps. Finally, the signal was inversely Fourier transformed back into the time domain. This signal contained only the bat call and was used for subsequent analysis. The FFT filter which removes noise may also inadvertently influence and change spectral call parameters. To test for this, we bootstrapped (Efron, 1979) calls from no-noise trials by estimating call parameters before and after layering artificial noise recorded on the same day as the randomly sampled call. Individual bootstrap replicates were performed by randomly sampling echolocation calls without replacement from no-noise trials, estimating click parameters from these, then layering noise on the signal waveform and applying the FFT filter and re-estimating call parameters. This was done with a signal-to-noise ratio (SNR) from 30 dB to 0 dB with a step size of 1 dB and 1000 bootstrap samples at each interval (Fig. S2).

Call parameter quantification

For each call, we defined the duration as the time interval between the −10 dB endpoints relative to the peak of the Hilbert envelope (the so-called D-duration). Received levels (RLs) were quantified as the RMS amplitude over the −10 dB duration. Call intervals were calculated as the time delay between the peak of the envelope of two consecutive calls. The SNR was quantified as the difference between the RMS received level and the RMS level of the first 125 ms of the sound file (in dB). A window length of 125 ms was chosen as a compromise between a long averaging window to mitigate the effects of potential transient peaks in the noise while avoiding overlap with the bat calls. SLs were calculated from RLs

Journal of Experimental Biology (2022) 225, jeb243917. doi:10.1242/jeb.243917

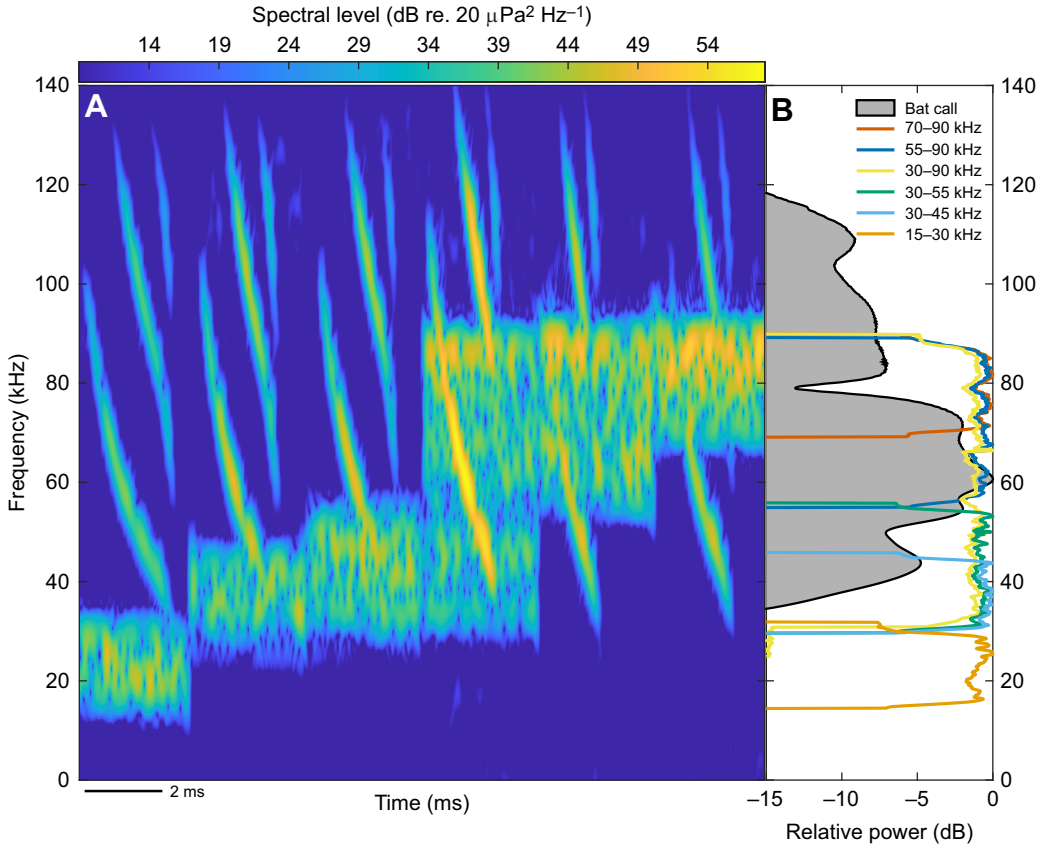

Fig. 3. Overview of noise band treatments and their relative overlap with echolocation calls of Daubenton's bats. (A) Example spectrograms of bat calls from the six different noise treatments: 15–30, 30–45, 30–55, 30–90, 55–90 and 70–90 kHz. Note how the third harmonic which is free from noise interference shows no sign of spectral shifts across treatment types. Spectrogram settings: sampling rate 400 kHz, chunk size 128 points, 97.5% overlap, Hann window, FFT size 1024 points (zero padding); frequency resolution 3.1 kHz; time resolution 8 µs. (B) Averaged relative power spectra of all bat calls from silent control trials (n=5205), and power spectra of the six noise bands as measured 1 m in front of the transducer (FFT size: 4000 points, sampling rate 400 kHz, frequency resolution 100 Hz).

by adding the transmission loss caused by spherical spreading ($20\log_{10}R$, where R is the range in meters, with a reference distance of 0.1 m) and the frequency-specific absorption (α, dB m^{-1}). We computed α for each bin in a power spectrum. The power spectrum was calculated using an FFT size of 4000 (bin width 100 Hz) and α was calculated for each bin [Bass et al. (1995), assuming an ambient temperature of 22°C, and the αR factor was multiplied with the linear spectrum, *sensu* Jakobsen et al. (2012). The concomitant effects of absorption across all frequencies can then be evaluated as the $10\log_{10}$ of the sum of all frequency bins of the corrected power spectrum (the 'area'), divided by the sum of all frequency bins of the uncorrected power spectrum. Evaluating absorption across all frequencies is important for frequency-modulated (FM) bat calls which span 10 s of kHz and thus is poorly represented by summary frequencies such as peak or centroid frequency estimates. The absorption factor on a dB scale was then added to the estimated SL. We also estimated peak, centroid frequency (defined as the sum of power per frequency bin multiplied by its corresponding bin divided by total spectrum power) and the half-power (−3 dB bandwidth).

Noise level quantification

The broadband RMS noise level as received by the bat was estimated from a known noise level of 72 dB re. 20 µPa RMS at 1 m by using spherical transmission loss and correcting the call for absorption as outlined in 'Call parameter quantification', above. Transmission loss characteristics of the transducer have been previously quantified (Foskolos et al., 2022) and were found to follow spherical transmission loss even down to ranges of 10 cm.

Statistics

We investigated the relationship between peak frequency, SL and noise bandwidth for the five loudest calls from each successful trial of the landing experiment. We used mixed effects models to account for autocorrelation of repeated measurements performed on the same bat and experimental day (Littell et al., 1998), and to avoid temporal autocorrelation such as acclimatization effects to noise over time. Mixed effects models (linear model, family=Gaussian, link=identity) were implemented using the lme4 package (v.1.1.2.6) (Bates et al., 2015) in R (v.4.0.3, www.r-project.org/), with P-values calculated using the Satterthwaite approximation for degrees of freedom implemented in the lmerTest package, v.3.1.3 (Kuznetsova et al., 2017). We made three different mixed effect models using (1) peak frequency, (2) SLs and (3) −3 dB spectral endpoints as response variables and noise band and noise level as fixed effects. Animal ID was treated as a fixed effect because of the low number of levels (<10) (Zuur et al., 2007).

Peak frequency as a function of noise band and level

To test whether peak frequency varied with emitted noise type, we modeled peak frequency as a function of noise band, animal ID and the received noise level with date and trial number as nested random effects on the intercept.

Journal of Experimental Biology (2022) 225, jeb243917. doi:10.1242/jeb.243917

Table 1. Number of successful trials the bats completed with signal-to-noise ratios (SNR) and source levels (SLs) for the different treatments

	Bat 1	Bat 2	Bat 3	Bat 4	Bat 5	$SNR_{RL–NL}$ (dB)	SL (dB re. 20 µPa RMS)
Control trials	207	221	206	203	204	34.4±5.1	107±3.6
15–30 kHz	49	49	48	48	46	10.6±2.8	109±3.2
30–45 kHz	41	42	42	41	41	14.7±3.1	113±2.9
30–55 kHz	39	41	40	41	41	16.5±3.3	115.1±2.6
30–90 kHz	40	41	40	40	41	23±3.7	115.5±3.2
55–90 kHz	40	41	40	40	40	24.4±3.5	112±3.6
70–90 kHz	40	42	41	39	39	22.9±3.3	110±7
Total no. of trials	456	477	457	452	452		

SNR of received calls and SLs are reported as means±s.d. Bat call SLs are referenced to 0.1 m. RL, received level; NL, noise level; RMS, root mean square.

Call amplitude as a function of noise band and level

The SL was modeled as a function of noise band, the $\log_{10}$ of distance, animal ID and an interaction term between noise band and emitted noise level [either 20 dB for silent controls *sensu* Foskolos et al. (2022) or 72 dB during noise] to allow for noise band-specific slopes, with date and trial number as nested random effects on the intercept. Modeling noise level with only two factors as opposed to a continuous variable circumvents the confounding effects of call SL decreasing during the approach phase while received noise level increases. This simpler approach to noise modeling more readily allows capture of the overall differences in potential SLs across noise treatments as compared with silent controls. Differences between slopes were calculated using the *lstrends* function implemented in the emmeans package (v.1.5.5.1) (https://CRAN.R-project.org/package=emmeans).

Half-power (−3 dB) spectral endpoints as a function of noise band

The spectral endpoints were individually modeled as a function of noise band and animal ID with the date and trial number as nested random effects on the intercept.

RESULTS

We recorded the vocalizations of five Daubenton's bats landing on a target emitting six different bandwidths of noise at the same source output level of 72 dB re. 20 µPa RMS at 1 m. In total, 2294 trials were carried out (Table 1).

We first tested the hypothesis that bats spectrally shift their calls when faced with different bands of masking noise. Despite the substantial potential for improving the ENR via the JAR (Fig. 1) in response to the low- and high-frequency noise bands, we found that none of them elicited a change in peak frequency with respect to silent control trials [Fig. 4A,B linear mixed effects model (LMEM),

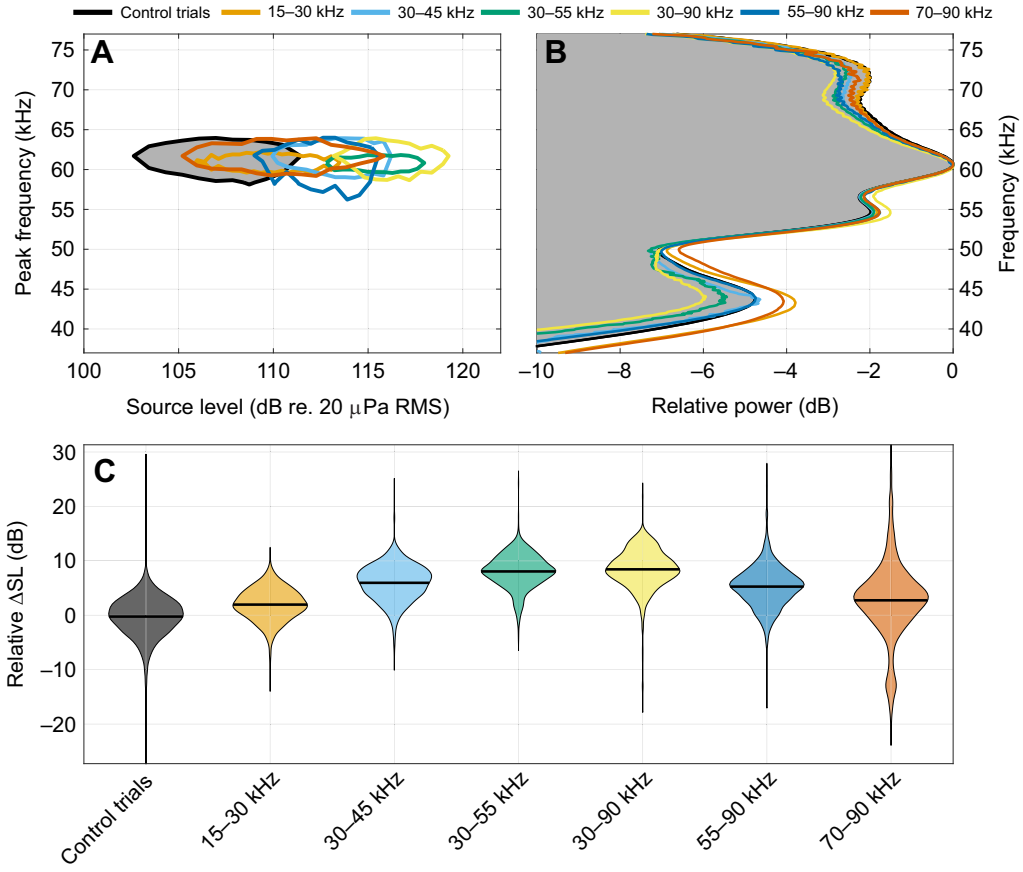

Fig. 4. Bats change their call SL but not peak frequency in response to masking noise. (A) Contour plots of peak frequency estimates as a function of SL for the different trial types. The increase in SL is larger for higher bandwidth masking noise, with no effect on the peak frequency of the call. (B) Averaged relative power spectra of bat calls for the different treatments. Shaded gray area indicates calls from control trials (FFT size 4000 points, sampling rate 400 kHz, frequency resolution 100 Hz). (C) Violin plots of relative change in SL for the noise treatments, scaled relative to the median call amplitude of each individual bat during control trials. Black line denotes mean values.

Journal of Experimental Biology (2022) 225, jeb243917. doi:10.1242/jeb.243917

Table 2. Statistical model for testing for changes in peak frequency

Covariates	Estimate±s.e.m.	d.f.	*t*-value	*P*-value
Intercept (Control trials, bat 1)	60.73±0.96	839.71	63.327	$<2\times10^{-16}$
15–30 kHz	2.87±1.68	10,618.96	1.710	0.0874
30–45 kHz	1.44±1.64	10,477.13	0.877	0.3803
30–55 kHz	1.00±1.63	10,432.22	0.614	0.5392
30–90 kHz	0.55±1.63	10,427.90	0.339	0.7344
55–90 kHz	0.43±1.60	10,366.57	0.270	0.7875
70–90 kHz	2.80±1.58	10,328.09	1.781	0.0750
Bat 2	0.34±0.48	2272.65	0.713	0.4757
Bat 3	−0.71±0.47	2279.88	−1.500	0.1337
Bat 4	−2.25±0.48	2278.93	−4.695	2.83×10^{-6}
Bat 5	−0.64±0.48	2274.78	−1.336	0.1818
NL	−0.02±0.03	11,362.36	−0.701	0.4835

Model<–peakfreq~noiseband+animal+noise level+(1|date/event).
Note that partial degrees of freedom arise as a consequence of the Satterthwaite approximation in which they are derived.

all noise band $P>0.05$ relative to control trials, Table 2, $N=2294$ trials].

The onset frequency of the half-power (−3 dB) bandwidth went from a bimodal distribution during control trials and the narrowband noise treatments, to a more truncated unimodal distribution for the widest noise band treatments (Fig. 5). Across all treatments, the half-power onset frequency decreased with respect to controls, and the response magnitude varied from 0.8 to 4 kHz (LMEM, $P<0.05$, Table S3). This shift in onset frequency arose as a passive consequence of increased SLs in response to noise, as the same truncated distribution appeared when comparing the 25% weakest amplitude calls from control trials with the 25% loudest calls from control trials (Fig. 6).

As no significant changes in peak frequency were observed for any of the noise bands, and the half-power bandwidth changed passively with call amplitude, we next tested our second hypothesis that the bats would defend their ENR by SL adjustments. We found that all bats increased their SL during noise exposure but to different extents. SL increased from 107±3.6 dB re. 20 µPa RMS (mean±s.d.) during control trials up to a maximum of 115.5±3.2 dB re. 20 µPa RMS in 30–90 kHz noise (Fig. 4A,C). The slopes (dB/dB noise) of the Lombard response were: 15–30 kHz, mean 0.05 (95% confidence interval, CI 0.04–0.06); 30–45 kHz, 0.12 (0.11–0.13); 30–55 kHz, 0.15 (0.14–0.16); 30–90 kHz, 0.17 (0.16–0.18); 55–90 kHz, 0.1 (0.096–0.114); and 70–90 kHz, 0.06 (0.05–0.07). All slopes were significantly different from each other (LMEM, $P<0.05$) except for 15–30/70–90 kHz and 30–45/55–90 kHz (LMEM, $P>0.05$, Tables S1 and S2).

To illustrate the sensitivity of spectral parameters to changes in SNR, we added varying noise levels to calls from control trials to reduce SNR in steps, allowing for examination of its effect on peak frequency and −3 dB spectral endpoint estimation (Fig. 7A). Next, to explore the low-pass filtering effects of changes in recording aspect of the acoustic axis, we plotted the average power spectrum of 1000 no-noise, on-axis calls recorded at approximately 1 m from the array, and the same calls as received on three other microphones, 0.6 m apart from the on-axis microphone, amounting to a 31 deg change in recording angle (Fig. 7B). Last, to demonstrate low-pass filtering effects of recording range we imposed several levels of absorption on the frequency-corrected spectrum of all on-axis no-noise calls (Fig. 7C) corresponding to four different target ranges of 1–10 m. All changes in recording conditions elicited a distortion of the apparent call spectrum through low-pass filtering effects, leading to substantially lower peak frequencies and shifts of the −3 dB spectral endpoints.

DISCUSSION

Echolocating bats must detect and process weak echoes to successfully navigate and forage. The ability to do so may be negatively affected by clutter (extraneous echoes not stemming from

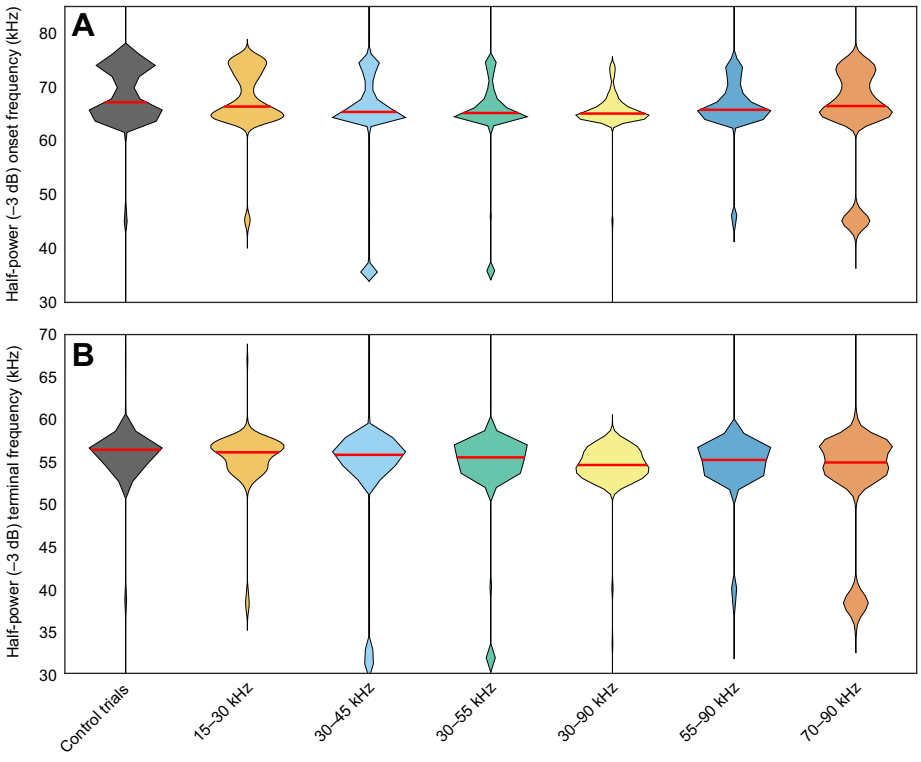

Fig. 5. Half-power (−3 dB) bandwidth onset and terminal frequencies for all calls. (A) Violin plots show onset frequencies are bimodal at the low source levels (SLs) seen in controls, and in response to 15–30 and 70–90 kHz noise masking bands. The upper part of the bimodal distribution becomes less prominent as the spectral peak is relatively more emphasized, as seen in averaged spectrograms (see Fig. 4B). (B) The terminal frequency is unimodal around 55 kHz. Red line indicates median.

Journal of Experimental Biology (2022) 225, jeb243917. doi:10.1242/jeb.243917

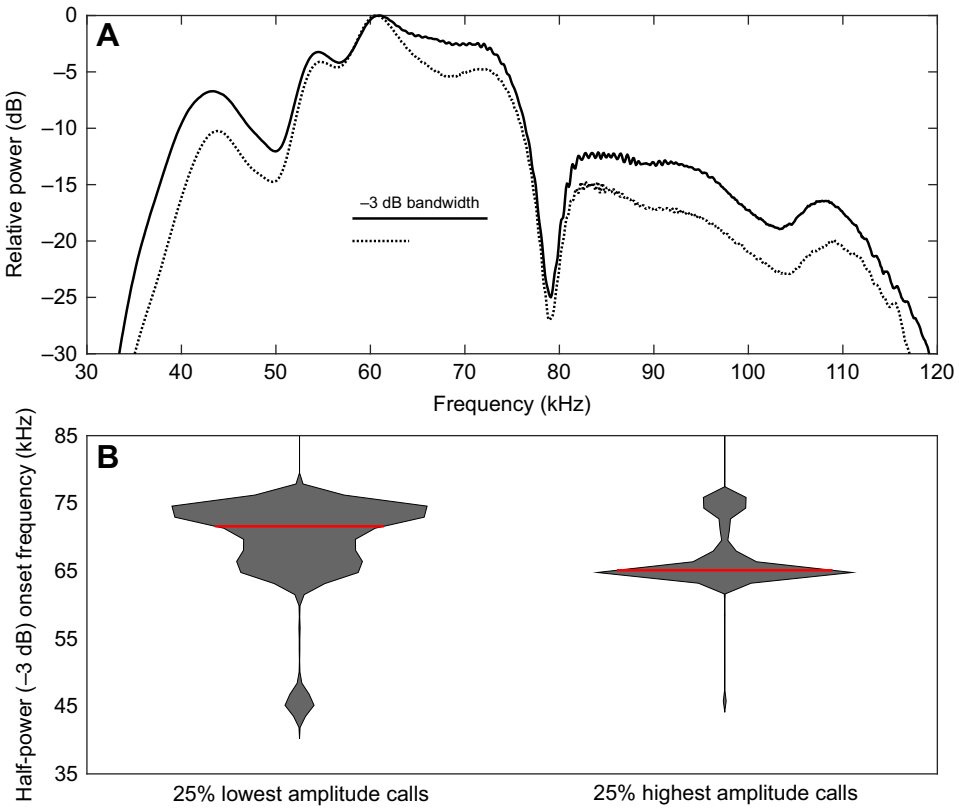

Fig. 6. The half-power bandwidth is affected by call amplitude. (A) Averaged power spectra of the 25% lowest amplitude calls (solid line) and 25% highest amplitude calls (dotted line). The peak of the power spectrum is relatively more prominent at high SLs. Horizontal bars indicate the −3 dB bandwidths. (B) From the more prominent peak follows a steeper relative fall off in power, and with it a decrease in the half-power onset frequency from 72.4 kHz for the low-amplitude calls to 64.1 kHz for the high-amplitude calls. This shift is independent of a spectral jamming avoidance response (JAR) and follows as a passive consequence of changes in call amplitude. Red line indicates median.

the target of interest) (Mao et al., 2016; Wheeler et al., 2016), masking from ambient noise (Foskolos et al., 2022) and jamming from sounds from prey or other bats (Corcoran and Conner, 2014). Inspired by electrical fish and motivated by the apparent problems that roosting and foraging bats may face when echolocating near other bats, a wealth of studies have sought to investigate how bats avoid jamming by spectrally shifting their call frequencies (Bates et al., 2008; Chiu et al., 2009; Gillam and Montero, 2016; Gillam et al., 2007; Habersetzer, 1981; Ibáñez et al., 2004; Necknig and Zahn, 2011; Obrist, 1995; Ratcliffe et al., 2004; Surlykke and Moss,

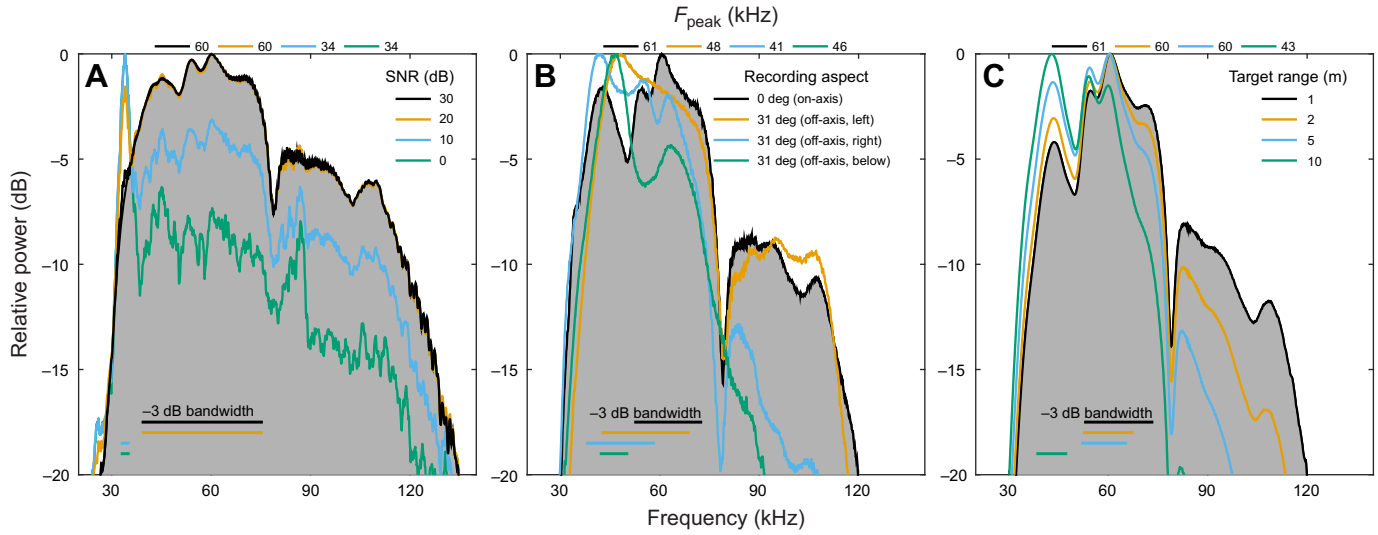

Fig. 7. Spectral parameter sensitivity to changes in signal-to-noise ratio (SNR), recording aspect and absorption. (A) Power spectrum of example calls from control trials with broadband 30–90 kHz noise layered at four SNRs. At low SNRs ≤10 dB, the main spectral peak at ∼60 kHz (seen at high SNRs ≥20 dB), and stable −3 dB spectral endpoints are de-emphasized and are replaced by a spectral peak and −3 dB endpoints from the 30–90 kHz masking noise. (B) Averaged relative power spectra of 1000 calls recorded at a distance of 0.96±0.2 m (mean±s.d.) from the target. At off-axis angles, the spectral peak and −3 dB endpoints shift by up to 20 kHz, and there is substantial low-pass filtering above 75 kHz. (C) Averaged relative power spectra of all bat calls from no-noise control trials (n=5205) with four levels of absorption imposed corresponding to distances of 1, 2, 5 and 10 m from the bat for a two-way absorption loss of 2, 4, 10 and 20 m. From frequency-specific absorption alone, the main spectral peak shifts from ∼60 kHz to ∼43 kHz at long ranges. The −3 dB onset frequency decreases gradually with longer ranges following the reduction in high-frequency acoustic energy, before both endpoints transition to the new spectral peak at 10 m. F_{peak} is peak frequency.

2000; Tressler and Smotherman, 2009; Ulanovsky et al., 2004). However, recording on-axis calls at known ranges from free-flying bats is difficult, both in the lab and in the wild. To accurately quantify the spectral content of on-axis calls, the location of the bat with respect to the receiver as well as the recording aspect to the center of the directional sound beam must be known. When these conditions are not met, it becomes difficult to ascertain what constitutes a spectral JAR, and what is potentially caused by spectral offsets from ambiguous recording range and aspect if the bat changes its flight pattern or acoustic beam pointing with respect to the recording microphone in response to noise (Fig. 7). While it is certainly possible that some bat species employ JAR via distinct spectral shifts in their vocal responses when faced with jamming, we note that most studies on JAR in bats have not employed a methodology that can exclude the possible effects of such low-pass filtering due to longer ranges and off-axis distortion (Mogensen and Møhl, 1979) in jamming situations compared with controls. Low-pass filtering effects from either aspect (Fig. 7B) or absorption alone (Fig. 7C) can change spectral parameters such as peak, band width and maximum frequencies by tens of kilohertz and hence easily be on a par with typical frequency shifts reported in JAR studies. It is therefore paramount for spectral parameter estimation of calls that the effects of call SNR, aspect and absorption are accounted for when testing for JAR.

In an attempt to avoid these experimental confounds, we here tested the hypothesis that bats, akin to electro-locating fish, avoid jamming by spectrally shifting the peak frequency of their calls away from band-limited noise. We did so by having Daubenton's bats land on a transducer target emitting noise of varying bandwidth offering no spatiotemporal masking release (Fig. 3). However, as the noise was band limited, substantial ENR improvement could be attained through spectral shifts – for example, moving peak call intensity out of the masking noise – provided that the decrease in noise level attained from a spectral masking release was not matched by an equivalent increase in detection threshold of the receiver in different parts of the audiogram. Many frequency-modulating bats (FM bats), including our study species, can indeed evoke such significant spectral shifts in their calls as they go through the search, approach or terminal buzz phases (Fig. 1). Despite this vocal plasticity, we found that the peak frequencies of the approach calls were remarkably stable for both controls and all bands of masking noise (Fig. 4A,B), leading us to reject the hypothesis that Daubenton's bats defend ENR through a spectral JAR. While peak frequency did not change across treatments, we found that the half-power (−3 dB) spectral endpoints were significantly different during noise exposure when compared with the no-noise control treatment (Table S3). However, this shift was unidirectional irrespective of the type of masking noise (Fig. 5; Table S3), showing that it is not driven by an effort to reduce spectral overlap with the masker. Instead, the same truncated distribution arises when comparing the 25% weakest calls with the 25% loudest from control trials (Fig. 6), suggesting that these spectral changes are driven by changes in call spectra with SL. Because their relative power is typically well below peak intensity, spectral endpoints are very sensitive to changes in SL and particularly vulnerable to low SNR, and we therefore caution against the use of spectral endpoints when investigating spectral JAR.

The lack of a spectral JAR is surprising as Daubenton's bats routinely drop their peak frequencies by almost an octave during buzzing (Fig. 1), probably through the concomitant effects of active tension release of the vocal folds (Ratcliffe et al., 2013) and lower driving pressures from the reduced call amplitude. Given the substantial ENR benefits of a JAR towards masking-free frequency bands, we speculate that the drop in peak frequency observed in buzz calls cannot be employed for biomechanical reasons when making approach phase calls where high SLs are required to render high enough echo returns – a hypothesis worth testing in future experiments.

Our rejection of the spectral shift JAR hypothesis is in support of the growing notion that bats perhaps do not commonly employ a spectral JAR to defend the ENR of returning echoes (Amichai et al., 2015; Cvikel et al., 2015; Götze et al., 2016). The lack of a spectral JAR also conforms with recent theoretical work which shows that a spectral JAR does not alleviate a jamming problem from other bats (Mazar and Yovel, 2020). However, how do bats then deal with jamming or masking? In contrast to a lack of spectral JAR, we found increasing SLs in response to the noise treatments (Fig. 4A,C; Table S3). This Lombard response was dependent on noise bandwidth with response magnitudes ranging from 0.05 dB/dB noise for the 15–30 kHz band to 0.17 dB/dB for the 30–90 kHz band, which is the frequency span of the first harmonic of the bat call (Fig. 3). A stronger Lombard response when exposed to broadband noise is consistent with Griffin et al.'s (1963) findings that broadband masking tasks are harder for bats. The magnitude of the Lombard response we observed is broadly similar to that of other mammals (Brumm et al., 2004; Cynx et al., 1998; Lane and Tranel, 1971; Luo et al., 2016; Sinnott et al., 1975) and birds (Brumm et al., 2009; Cynx et al., 1998; Schuster et al., 2012), which ranges from 0.05 to 0.7 dB/dB of noise. Thus, in spite of compensations to noise being commonplace, they are typically well below perfect 1 dB/dB compensation, resulting in reduced ENR and communication ranges.

A Lombard response elicited by broadband noise has been documented in bats before (Foskolos et al., 2022; Lu et al., 2020; Luo et al., 2016). Additionally, noise that is band limited and does not overlap has been shown to elicit a weaker Lombard response as compared with broadband noise, which does spectrally overlap with echolocation calls (Lu et al., 2020; Luo et al., 2016). We find the same, more modest Lombard response to noise outside the frequency span of echolocation calls (Fig. 4A,C). Curiously, the Lombard response is of the same magnitude (i.e. not statistically different) in 15–30 kHz noise (average slope of 0.05 dB/dB) as it is in 70–90 kHz noise (average slope of 0.06 dB/dB; Tables S1 and S2). This is in spite of 15–30 kHz noise being an octave below the peak frequency (∼60 kHz) of the approach calls and terminating 4 kHz below the peak frequency of buzz calls (Fig. 1), whereas 70–90 kHz noise onsets within 10 kHz of peak frequencies typical of approach calls (Fig. 3). If the higher frequency part of their echolocation calls is necessary for echo-guided landing on the target transducer, 70–90 kHz noise should, all else being equal, exert a more adverse effect on echo detectability, but in spite of this, call adjustments for the two noise bands are the same. This suggests that the Lombard response is a rather simple reflexive adjustment which serves to imperfectly defend ENR. It also implies that for bats, the magnitude of the Lombard response is driven by perceived loudness through the concomitant effects of total noise bandwidth (see also Lu et al., 2020; Luo et al., 2016) and level (Foskolos et al., 2022) and less by the actual spectral overlap with the returning echo of interest. Thus, our results suggest that the Lombard response is the result of a direct auditory assessment of the noise load rather than an evaluation of the actual ENR of the returning echoes.

For bats echolocating in the vicinity of other calling bats, the alleviation of jamming effects may also occur through simple spatial

avoidance, as exposure to loud calls from conspecifics is unlikely to have a bearing on post-exposure performance (Hom et al., 2016; Simmons et al., 2018). This resilience to performance reduction is probably due to the lack of an apparent detection threshold shift after noise exposure (Simmons et al., 2015). Additionally, bats can reduce the extent of temporal overlap through timing changes of outgoing acoustic signals. Such temporal jamming avoidance, where bats desynchronize outgoing calls from those of nearby conspecifics through changes in either call duration or calling interval have been observed for several species (Obrist, 1995), and in huge flocks, jamming may be effectively mitigated when bats on average reduce calling rate (Beleyur and Goerlitz, 2019). Lastly, actively increasing call amplitude through a Lombard response will, when loud enough, incur added energetic costs for bats (Currie et al., 2020). Given that spatial avoidance and desynchronization of call timing probably incur no added energetic costs, a Lombard response should thus be expected to serve as a last resort method of defending ENR.

Conclusion

We show that Daubenton's bats in a landing task do not exhibit a spectral JAR, in spite of their vocal ability to adjust peak frequencies by almost an octave in the transition from approach to buzz calls. Instead, Daubenton's bats partially defend ENRs through a Lombard response. This response is dependent on total noise bandwidth and appears to be at least partially decoupled from the spectral overlap of noise with echolocation calls, suggesting that the Lombard response is a reflexive change rather than a conscious vocal adjustment to ENR changes. How bats deal with echolocation calls of conspecifics or jamming signals from prey items is still not fully resolved but given the growing body of evidence suggesting that bats do not employ a spectral JAR, we posit that bats principally ameliorate conspecific jamming (i) by spatial avoidance, thereby reducing the jamming problem for both bats, (ii) through reduction of temporal overlap via changes in call timing and duration when possible and (iii) via an increase in call amplitude when acoustic overlap is unavoidable.

Acknowledgements

We thank Aleksandrina Mitseva, Per Guldhammer Henriksen and Marie Rosenkjær Skalshøi for dedicated assistance during animal training and data collection. We thank Jamie Macaulay for help with PAMGuard and development of tools for extraction of detected calls to MATLAB.

Competing interests

The authors declare no competing or financial interests.

Author contributions

Conceptualization: M.B.P., K.B., P.T.M.; Methodology: M.B.P., I.F., P.T.M.; Software: K.B., I.F.; Validation: M.B.P.; Formal analysis: M.B.P., K.B., I.F.; Investigation: M.B.P., A.S.U.; Resources: M.B.P., P.T.M.; Data curation: M.B.P.; Writing - original draft: M.B.P., L.S., P.T.M.; Writing - review & editing: M.B.P., A.S.U., K.B., I.F., L.S., P.T.M.; Visualization: M.B.P., L.S.; Supervision: P.T.M.; Project administration: P.T.M.; Funding acquisition: P.T.M.

Funding

This research was funded by a large frame grant from the Danish Council for Independent Research, Natural Sciences (Natur og Univers, Det Frie Forskningsråd, FNU) to P.T.M.

Data availability

Data used in this article are available from the Open Science Framework: https://osf.io/t2rbe/ (doi:10.17605/OSF.IO/T2RBE).

References

Amichai, E., Blumrosen, G. and Yovel, Y. (2015). Calling louder and longer: how bats use biosonar under severe acoustic interference from other bats. *Proc. R. Soc. Lond. B Biol. Soc.* **282**, 20152064. doi:10.1098/rspb.2015.2064

Au, W. W. L. (1993). *The Sonar of Dolphins*. New York, NY: Springer.

Au, W. W. L., Branstetter, B., Moore, P. W. and Finneran, J. J. (2012). Dolphin biosonar signals measured at extreme off-axis angles: insights to sound propagation in the head. *J. Acoust. Soc. Am.* **132**, 1199-1206. doi:10.1121/1.4730901

Bass, H. E., Sutherland, L. C., Zuckerwar, A. J., Blackstock, D. T. and Hester, D. M. (1995). Atmospheric absorption of sound: further developments. *J. Acoust. Soc. Am.* **97**, 680-683. doi:10.1121/1.412989

Bates, M. E., Stamper, S. A. and Simmons, J. A. (2008). Jamming avoidance response of big brown bats in target detection. *J. Exp. Biol.* **211**, 106-113. doi:10.1242/jeb.009688

Bates, D., Mächler, M., Bolker, B. and Walker, S. (2015). Fitting linear mixed-effects models using lme4. *J. Stat. Softw.* **67**, 1-48. doi:10.18637/jss.v067.i01

Beleyur, T. and Goerlitz, H. R. (2019). Modeling active sensing reveals echo detection even in large groups of bats. *Proc. Natl. Acad. Sci. USA.* **116**, 26662-26668. doi:10.1073/pnas.1821722116

Brumm, H., Voss, K., Köllmer, I. and Todt, D. (2004). Acoustic communication in noise: regulation of call characteristics in a New World monkey. *J. Exp. Biol.* **207**, 443. doi:10.1242/jeb.00768

Brumm, H., Schmidt, R. and Schrader, L. (2009). Noise-dependent vocal plasticity in domestic fowl. *Anim. Behav.* **78**, 741-746. doi:10.1016/j.anbehav.2009.07.004

Bullock, T. H., Hamstra, R. H. and Scheich, H. (1972). The jamming avoidance response of high frequency electric fish. *J. Comp. Physiol.* **77**, 1-22. doi:10.1007/BF00696517

Chiu, C., Xian, W. and Moss, C. F. (2009). Adaptive echolocation behavior in bats for the analysis of auditory scenes. *J. Exp. Biol.* **212**, 1392-1404. doi:10.1242/jeb.027045

Corcoran, A. J. and Conner, W. E. (2014). Bats jamming bats: food competition through sonar interference. *Science* **346**, 745-747. doi:10.1126/science.1259512

Currie, S. E., Boonman, A., Troxell, S., Yovel, Y. and Voigt, C. C. (2020). Echolocation at high intensity imposes metabolic costs on flying bats. *Nat. Ecol. Evol.* **4**, 1174-1177. doi:10.1038/s41559-020-1249-8

Cvikel, N., Levin, E., Hurme, E., Borissov, I., Boonman, A., Amichai, E. and Yovel, Y. (2015). On-board recordings reveal no jamming avoidance in wild bats. *Proc. Biol. Sci.* **282**, 20142274. doi:10.1098/rspb.2014.2274

Cynx, J., Lewis, R., Tavel, B. and Tse, H. (1998). Amplitude regulation of vocalizations in noise by a songbird, *Taeniopygia guttata*. *Anim. Behav.* **56**, 107-113. doi:10.1006/anbe.1998.0746

Efron, B. (1979). Bootstrap methods: another look at the jackknife. *Ann. Stat.* **7**, 1-26. doi:10.1214/aos/1176344552

Foskolos, I., Pedersen, M. B., Beedholm, K., Uebel, A. S., Macaulay, J., Stidsholt, L., Brinkløv, S. and Madsen, P. T. (2022). Echolocating Daubenton's bats are resilient to broadband, ultrasonic masking noise during active target approaches. *J. Exp. Biol.*, **225**, jeb242957. doi:10.1242/jeb.242957

Gillam, E. H. and Montero, B. K. (2016). Influence of call structure on the jamming avoidance response of echolocating bats. *J. Mammal.* **97**, 14-22. doi:10.1093/jmammal/gyv147

Gillam, E. H., Ulanovsky, N. and McCracken, G. F. (2007). Rapid jamming avoidance in biosonar. *Proc. Biol. Sci.* **274**, 651-660. doi:10.1098/rspb.2006.0047

Gillespie, D., Mellinger, D. K., Gordon, J., McLaren, D., Redmond, P., McHugh, R., Trinder, P., Deng, X. Y. and Thode, A. (2009). PAMGUARD: semiautomated, open source software for real-time acoustic detection and localization of cetaceans. *J. Acoust. Soc. Am.* **125**, 2547-2547. doi:10.1121/1.4808713

Götze, S., Koblitz, J. C., Denzinger, A. and Schnitzler, H.-U. (2016). No evidence for spectral jamming avoidance in echolocation behavior of foraging pipistrelle bats. *Sci. Rep.* **6**, 30978. doi:10.1038/srep30978

Griffin, D. R. (1958). *Listening in the Dark: The Acoustic Orientation of Bats and Men*. Oxford, England: Yale University Press.

Griffin, D. R. and Galambos, R. (1940). Obstacle avoidance by flying bats. *Anat. Rec.* **79**, 95.

Griffin, D. R. and Galambos, R. (1941). The sensory basis of obstacle avoidance by flying bats. *J. Exp. Zool.* **86**, 481-506. doi:10.1002/jez.1400860310

Griffin, D. R., McCue, J. J. G. and Grinnell, A. D. (1963). The resistance of bats to jamming. *J. Exp. Zool.* **152**, 229-250. doi:10.1002/jez.1401520303

Habersetzer, J. (1981). Adaptive echolocation sounds in the bat *Rhinopoma hardwickei*. *J. Comp. Physiol.* **144**, 559-566. doi:10.1007/BF01326841

Hom, K. N., Linnenschmidt, M., Simmons, J. A. and Simmons, A. M. (2016). Echolocation behavior in big brown bats is not impaired after intense broadband noise exposures. *J. Exp. Biol.* **219**, 3253-3260. doi:10.1242/jeb.143578

Ibáñez, C., Juste, J., López-Wilchis, R. and Núñez-Garduño, A. (2004). Habitat variation and jamming avoidance in echolocation calls of the Sac-winged Bat (*Balantiopteryx plicata*). *J. Mammal.* **85**, 38-42. doi:10.1644/1545-1542(2004)085<0038:HVAJAI>2.0.CO;2

Jakobsen, L., Kalko, E. K. V. and Surlykke, A. (2012). Echolocation beam shape in emballonurid bats, *Saccopteryx bilineata* and *Cormura brevirostris*. *Behav. Ecol. Sociobiol.* **66**, 1493-1502. doi:10.1007/s00265-012-1404-6

Jones, T. K., Allen, K. M. and Moss, C. F. (2021). Communication with self, friends and foes in active-sensing animals. *J. Exp. Biol.* **224**, jeb242637. doi:10.1242/jeb.242637

Kuznetsova, A., Brockhoff, P. B. and Christensen, R. H. B. (2017). lmerTest package: tests in linear mixed effects models. *J. Stat. Softw.* **82**, 1-26. doi:10.18637/jss.v082.i13
Kyhn, L. A., Tougaard, J., Jensen, F., Wahlberg, M., Stone, G., Yoshinaga, A., Beedholm, K. and Madsen, P. T. (2009). Feeding at a high pitch: source parameters of narrow band, high-frequency clicks from echolocating off-shore hourglass dolphins and coastal Hector's dolphins. *J. Acoust. Soc. Am.* **125**, 1783-1791. doi:10.1121/1.3075600
Lane, H. and Tranel, B. (1971). The lombard sign and the role of hearing in speech. *J. Speech Hear. Res.* **14**, 677-709. doi:10.1044/jshr.1404.677
Littell, R. C., Henry, P. R. and Ammerman, C. B. (1998). Statistical analysis of repeated measures data using SAS procedures. *J. Anim. Sci.* **76**, 1216-1231. doi:10.2527/1998.7641216x
Lombard, E. (1911). Le signe de l'élévation de la voix. *Annales des Maladies de l'Oreille, du Larynx du Nez et du Pharynx* **37**, 101-119.
Lu, M., Zhang, G. and Luo, J. (2020). Echolocating bats exhibit differential amplitude compensation for noise interference at a sub-call level. *J. Exp. Biol.* **223**, jeb225284. doi:10.1242/jeb.225284
Luo, J. and Moss, C. F. (2017). Echolocating bats rely on audiovocal feedback to adapt sonar signal design. *Proc. Natl. Acad. Sci. USA* **114**, 10978-10983. doi:10.1073/pnas.1711892114
Luo, J., Goerlitz, H. R., Brumm, H. and Wiegrebe, L. (2016). Linking the sender to the receiver: vocal adjustments by bats to maintain signal detection in noise. *Sci. Rep.* **5**, 18556. doi:10.1038/srep18556
Macaulay, J., Gordon, J., Gillespie, D., Malinka, C. and Northridge, S. (2017). Passive acoustic methods for fine-scale tracking of harbour porpoises in tidal rapids. *J. Acoust. Soc. Am.* **141**, 1120-1132. doi:10.1121/1.4976077
Mao, B., Aytekin, M., Wilkinson, G. S. and Moss, C. F. (2016). Big brown bats (*Eptesicus fuscus*) reveal diverse strategies for sonar target tracking in clutter. *J. Acoust. Soc. Am.* **140**, 1839-1849. doi:10.1121/1.4962496
Mazar, O. and Yovel, Y. (2020). A sensorimotor model shows why a spectral jamming avoidance response does not help bats deal with jamming. *eLife* **9**, e55539. doi:10.7554/eLife.55539
Mogensen, F. and Møhl, B. (1979). Sound radiation patterns in the frequency domain of cries from a Vespertilionid bat. *J. Comp. Physiol.* **134**, 165-171. doi:10.1007/BF00610475
Møhl, B. (1988). Target detection by echolocating bats. In *Animal Sonar: Processes and Performance* (ed. P. E. Nachtigall and P. W. B. Moore), pp. 435-450. Boston, MA: Springer US.
Necknig, V. and Zahn, A. (2011). Between-species jamming avoidance in pipistrelles? *J. Comp. Physiol. A Neuroethol. Sens. Neural Behav. Physiol.* **197**, 469-473. doi:10.1007/s00359-010-0586-5
Nelder, J. A. and Mead, R. (1965). A simplex method for function minimization. *Comput. J.* **7**, 308-313. doi:10.1093/comjnl/7.4.308
Obrist, M. K. (1995). Flexible bat echolocation: the influence of individual, habitat and conspecifics on sonar signal design. *Behav. Ecol. Sociobiol.* **36**, 207-219. doi:10.1007/BF00177798
Ratcliffe, J. M., Hofstede, H. M. t., Avila-Flores, R., Fenton, M. B., McCracken, G. F., Biscardi, S., Blasko, J., Gillam, E., Orprecio, J. and Spanjer, G. (2004). Conspecifics influence call design in the Brazilian free-tailed bat, *Tadarida brasiliensis*. *Can. J. Zool.* 82, 966-971. doi:10.1139/z04-074
Ratcliffe, J. M., Elemans, C. P. H., Jakobsen, L. and Surlykke, A. (2013). How the bat got its buzz. *Biol. Lett.* **9**, 20121031. doi:10.1098/rsbl.2012.1031
Scheich, H. (1977). Neural basis of communication in the high frequency electric fish,Eigenmannia virescens (jamming avoidance response). *J. Comp. Physiol.* **113**, 181-206. doi:10.1007/BF00611988
Schuster, S., Zollinger, S. A., Lesku, J. A. and Brumm, H. (2012). On the evolution of noise-dependent vocal plasticity in birds. *Biol. Lett.* **8**, 913-916. doi:10.1098/rsbl.2012.0676
Simmons, A. M., Boku, S., Riquimaroux, H. and Simmons, J. A. (2015). Auditory brainstem responses of Japanese house bats (*Pipistrellus abramus*) after exposure to broadband ultrasonic noise. *J. Acoust. Soc. Am.* **138**, 2430-2437. doi:10.1121/1.4931901
Simmons, A. M., Ertman, A., Hom, K. N. and Simmons, J. A. (2018). Big brown bats (*Eptesicus fuscus*) successfully navigate through clutter after exposure to intense band-limited sound. *Sci. Rep.* **8**, 13555. doi:10.1038/s41598-018-31872-x
Sinnott, J. M., Stebbins, W. C. and Moody, D. B. (1975). Regulation of voice amplitude by the monkey. *J. Acoust. Soc. Am.* **58**, 412-414. doi:10.1121/1.380685
Smith, A. B., Pacini, A. F., Nachtigall, P. E., Laule, G. E., Aragones, L. V., Magno, C. and Suarez, L. J. A. (2019). Transmission beam pattern and dynamics of a spinner dolphin (*Stenella longirostris*). *J. Acoust. Soc. Am.* **145**, 3595-3605. doi:10.1121/1.5111347
Stidsholt, L., Müller, R., Beedholm, K., Ma, H., Johnson, M. and Madsen, P. T. (2020). Energy compensation and received echo level dynamics in constant-frequency bats during active target approaches. *J. Exp. Biol.* **223**, jeb217109. doi:10.1242/jeb.217109
Surlykke, A. and Moss, C. F. (2000). Echolocation behavior of big brown bats, Eptesicus fuscus, in the field and the laboratory. *J. Acoust. Soc. Am.* **108**, 2419-2429. doi:10.1121/1.1315295
Takahashi, E., Hyomoto, K., Riquimaroux, H., Watanabe, Y., Ohta, T. and Hiryu, S. (2014). Adaptive changes in echolocation sounds by *Pipistrellus abramus* in response to artificial jamming sounds. *J. Exp. Biol.* **217**, 2885-2891. doi:10.1242/jeb.101139
Tressler, J. and Smotherman, M. S. (2009). Context-dependent effects of noise on echolocation pulse characteristics in free-tailed bats. *J. Comp. Physiol. A Neuroethol. Sens. Neural Behav. Physiol.* **195**, 923-934. doi:10.1007/s00359-009-0468-x
Ulanovsky, N., Fenton, M. B., Tsoar, A. and Korine, C. (2004). Dynamics of jamming avoidance in echolocating bats. *Proc. R. Soc. Lond. B Biol. Sci.* **271**, 1467-1475. doi:10.1098/rspb.2004.2750
Wheeler, A. R., Fulton, K. A., Gaudette, J. E., Simmons, R. A., Matsuo, I. and Simmons, J. A. (2016). Echolocating big brown bats, *Eptesicus fuscus*, modulate pulse intervals to overcome range ambiguity in cluttered surroundings. *Front. Behav. Neurosci.* **10**, 125. doi:10.3389/fnbeh.2016.00125
Zuur, A., Ieno, E. and Smith, G. (2007). *Analysing Ecological Data*. Springer-Verlag.

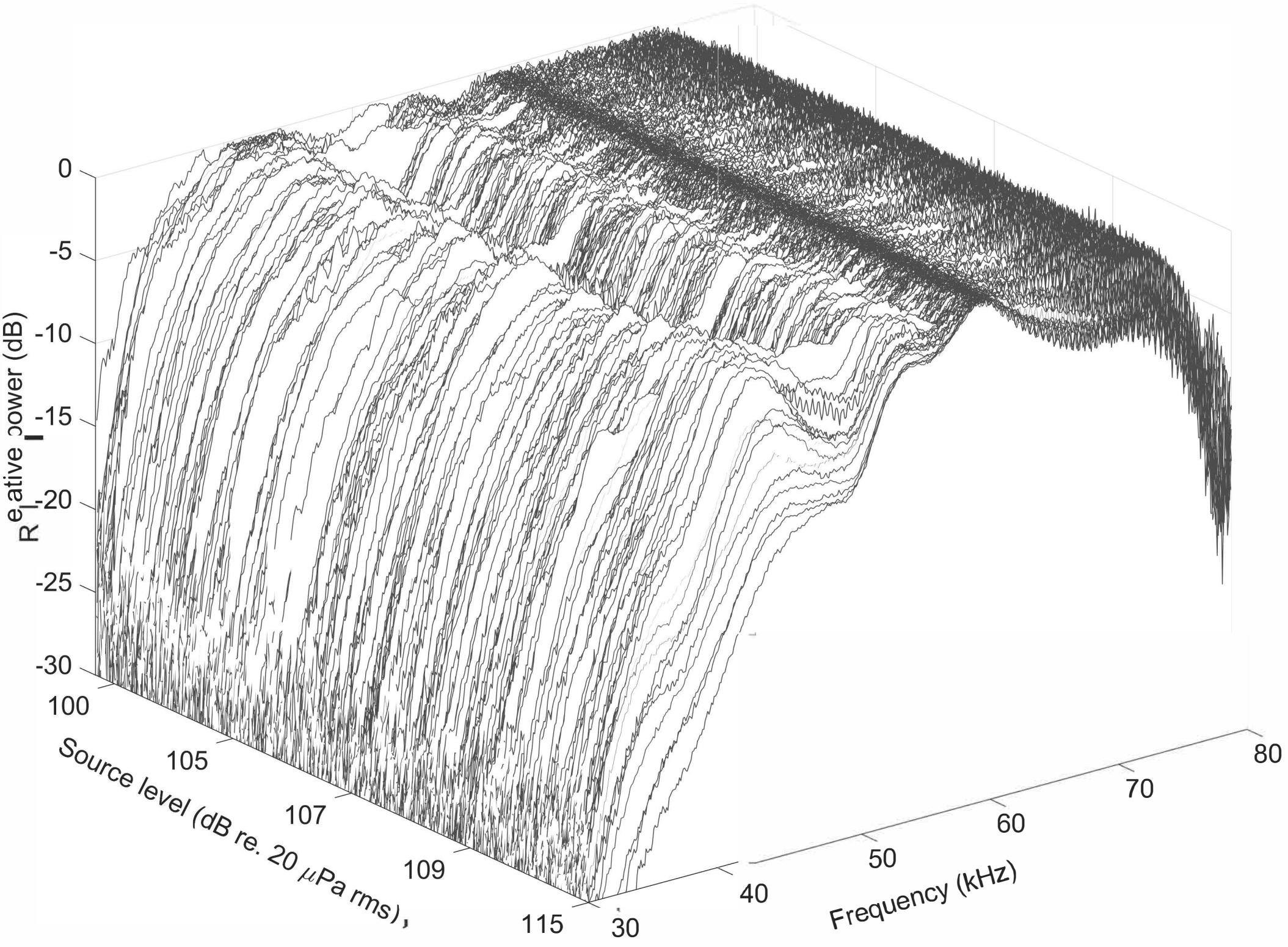

Fig. S1. Waterfall plot of all call power spectra from control trials. With the possible exception of a modest relative deemphasis of the spectral peak at ≈43 kHz at very high source levels, no significant changes occur in the spectrum across the range of source levels emitted in control trials (n = 5205).

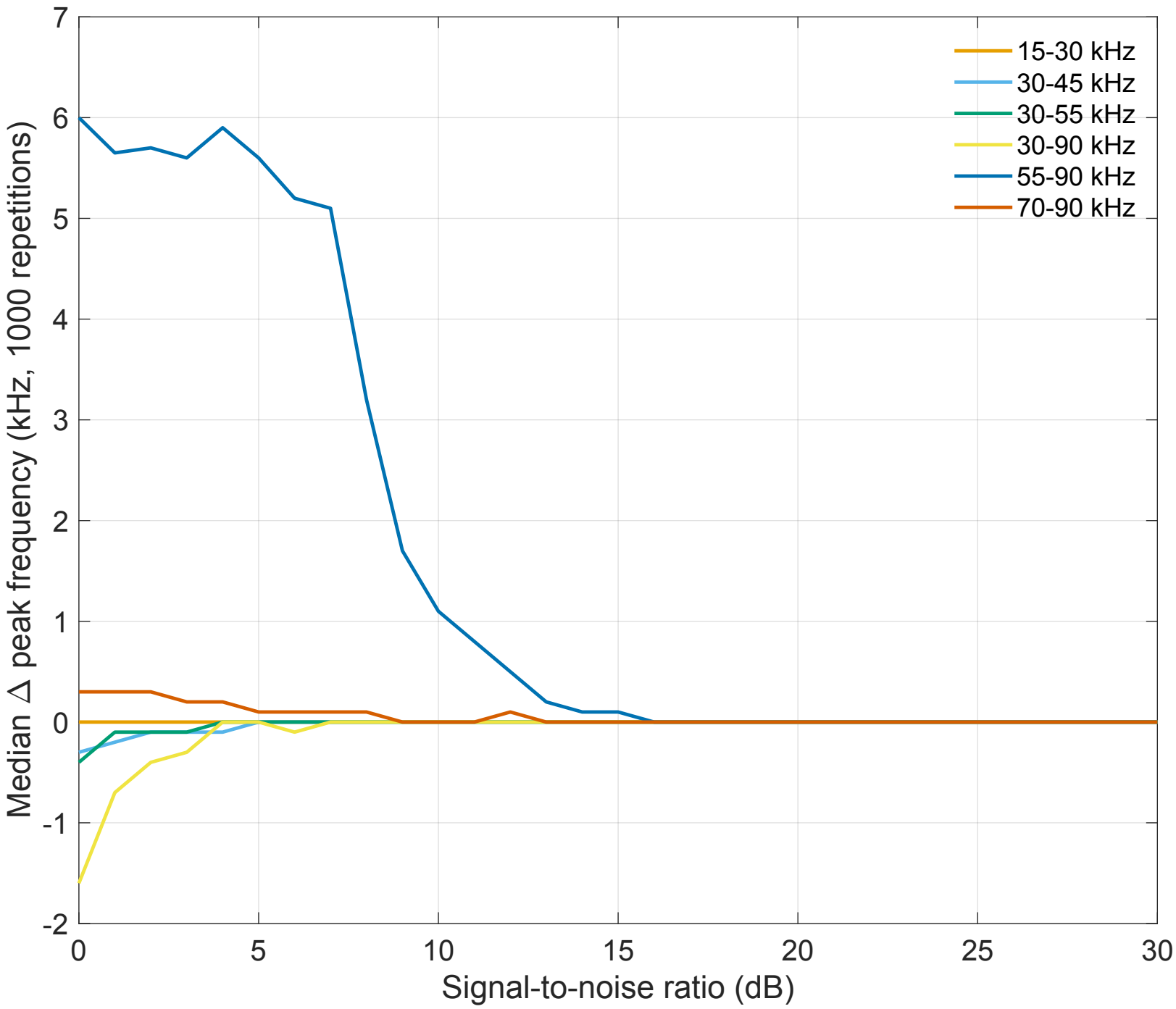

Fig. S2. Median Δ peak frequency estimate before and after artificially layering noise. The efficacy of the FFT-filter noise removal remains high for 5 of the 6 noise-bands down to an SNR of ≈5 dB, but tapers off at ≈15 dB for the 55-90 kHz noise. For all treatments, the median threshold for when deviations in estimated peak frequencies occur is well below average SNR (**Fejl! Henvisningskilde ikke fundet.**).

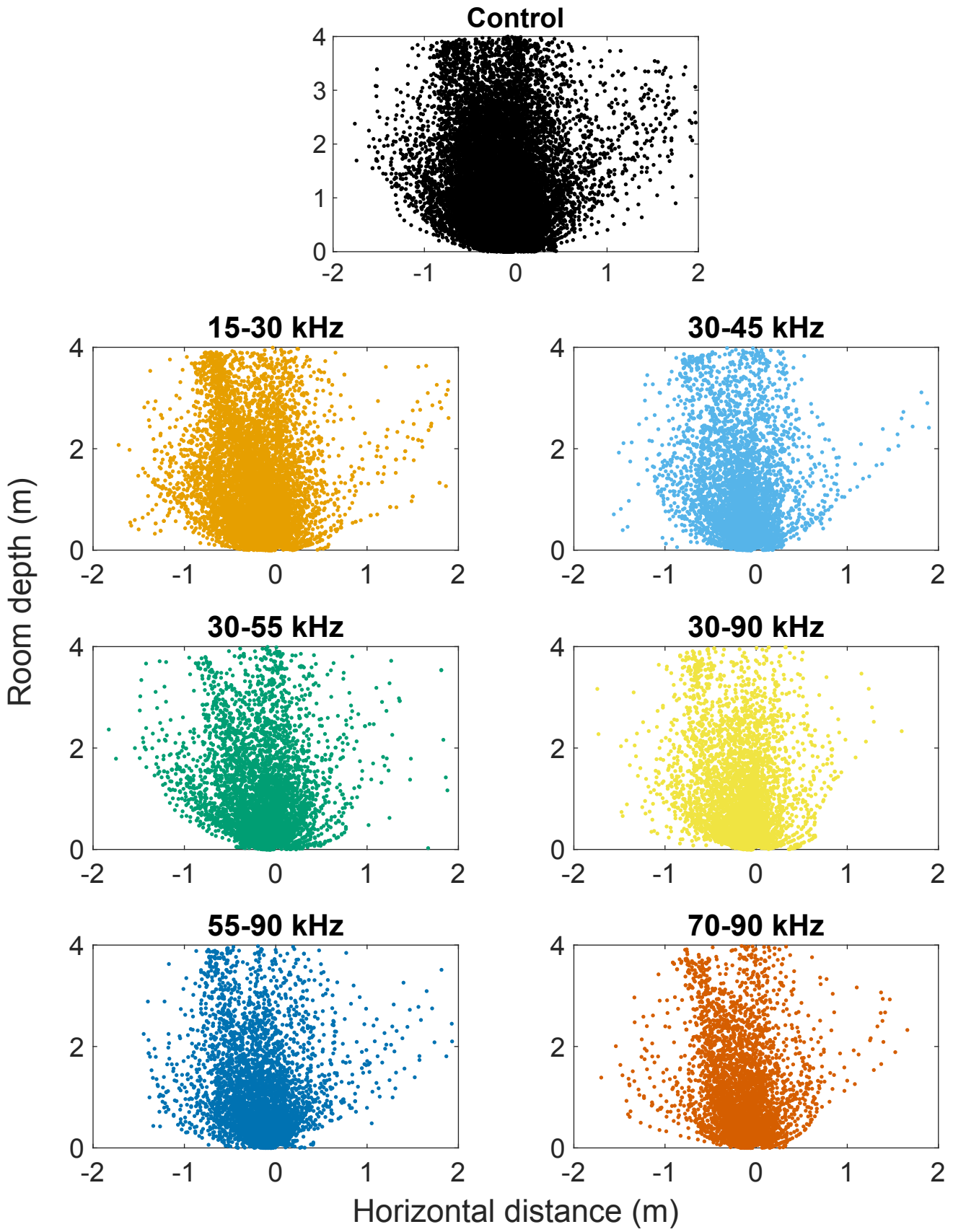

Fig. S3. Localized tracks of all flight paths. The bats directly approach the target (coordinates 0,0) and the path chosen does not deviate from control across treatments.

Table S1. Statistical models for changes in Source level when exposed to masking noise.

Model <- SL ~ noiseband + $\log_{10}$(distance) + animal + noise level:noiseband + (1|date/event)				
Covariates	**Estimate ± s.e.m.**	**df**	**t-value**	**p-value**
Intercept (15-30 kHz, bat #1)	102.99 ± 0.31	257.44	329.738	$< 2{\cdot}10^{-16}$
30-45 kHz	-1.08 ± 0.36	2177.49	-2.963	$3.08{\cdot}10^{-3}$
30-55 kHz	-1.67 ± 0.36	2177.52	-4.601	$4.438{\cdot}10^{-6}$
30-90 kHz	-2.48 ± 0.36	2177.88	-6.792	$1.4231{\cdot}10^{-11}$
55-90 kHz	-0.93 ± 0.36	2177.80	-2.585	$9.8{\cdot}10^{-3}$
70-90 kHz	-0.18 ± 0.37	2178.21	-0.485	0.62761
$\log_{10}$(distance)	11.38 ± 0.15	10613.74	77.401	$< 2{\cdot}10^{-16}$
Bat #2	-1.65 ± 0.16	2182.93	-10.484	$< 2{\cdot}10^{-16}$
Bat #3	-1.15 ± 0.156	2185.28	-7.408	$1.83{\cdot}10^{-13}$
Bat #4	-0.37 ± 0.16	2186.57	-2.363	$1.822{\cdot}10^{-2}$
Bat #5	-0.98 ± 0.16	2184.99	-6.111	$5.8162{\cdot}10^{-10}$
15-30 kHz : noise level	0.05 ± 0.005	2190.82	11.368	$< 2{\cdot}10^{-16}$
30-45 kHz : noise level	0.12 ± 0.005	2179.00	24.793	$< 2{\cdot}10^{-16}$
30-55 kHz : noise level	0.15 ± 0.005	2178.32	32.202	$< 2{\cdot}10^{-16}$
30-90 kHz : noise level	0.17 ± 0.005	2179.50	36.473	$< 2{\cdot}10^{-16}$
55-90 kHz : noise level	0.10 ± 0.005	2178.23	22.488	$< 2{\cdot}10^{-16}$
70-90 kHz : noise level	0.06 ± 0.005	2178.36	12.364	$< 2{\cdot}10^{-16}$

Table S2. Contrasts in slopes across noise treatments. Results are averaged over the levels of: animal & noise level. P-values are adjusted with the Tukey method for comparing a family of 6 estimates.

model.trends<-lstrends(mymodel, "noiseband", var="noiselevel")				
Contrasts	**Estimate ± s.e.m.**	**df**	**t-ratio**	**p-value**
15-30 kHz : 30-45 kHz	-0.06 ± 0.007	2182	-9.814	<.0001
15-30 kHz : 30-55 kHz	-0.099 ± 0.007	2182	-15.186	<.0001
15-30 kHz : 30-90 kHz	-0.12 ± 0.007	2182	-18.325	<.0001
15-30 kHz : 55-90 kHz	-0.05 ± 0.007	2182	-8.033	<.0001
15-30 kHz : 70-90 kHz	-0.008 ± 0.007	2183	-1.183	0.8450
30-45 kHz : 30-55 kHz	-0.04 ± 0.007	2177	-5.319	<.0001
30-45 kHz : 30-90 kHz	-0.06 ± 0.007	2177	-8.438	<.0001
30-45 kHz : 55-90 kHz	0.01 ± 0.007	2177	1.804	0.4631
30-45 kHz : 70-90 kHz	0.06 ± 0.007	2177	8.463	<.0001
30-55 kHz : 30-90 kHz	-0.02 ± 0.007	2177	-3.121	0.0225
30-55 kHz : 55-90 kHz	0.05 ± 0.007	2177	7.146	<.0001
30-55 kHz : 70-90 kHz	0.09 ± 0.007	2177	13.734	<.0001
30-90 kHz : 55-90 kHz	0.07 ± 0.007	2177	10.275	<.0001
30-90 kHz : 70-90 kHz	0.11 ± 0.007	2177	16.822	<.0001
55-90 kHz : 70-90 kHz	0.04 ± 0.007	2177	6.709	<.0001

Table S3. Statistical models for changes in half-power onset and terminal frequencies when exposed to masking noise.

-3dB onset frequency ~ noiseband + animal + (1 | date/event)				
	Mean ± s.e.m	df	t-ratio	p-value
Intercept (Control trials, bat #1)	71.32 ± 0.27	61.78	265.25	$<2 \cdot 10^{-16}$
15-30 kHz	-0.83 ± 0.31	2232.31	-2.65	0.008
30-45 kHz	-3.98 ± 0.33	2285.20	-12.21	$<2 \cdot 10^{-16}$
30-55 kHz	-3.16 ± 0.33	2275.86	-9.58	$<2 \cdot 10^{-16}$
30-90 kHz	-3.17 ± 0.33	2275.77	-9.63	$<2 \cdot 10^{-16}$
55-90 kHz	-1.98 ± 0.33	2274.94	-5.99	$2.4 \cdot 10^{-9}$
70-90 kHz	-2.57 ± 0.33	1174.78	-7.79	$1.05 \cdot 10^{-14}$
Bat #2	-0.55 ± 0.28	2270.12	-1.95	0.051
Bat #3	-3.56 ± 0.28	2268.12	-12.7	$<2 \cdot 10^{-16}$
Bat #4	-6.05 ± 0.28	2268.33	-21.23	$<2 \cdot 10^{-16}$
Bat #5	-2.45 ± 0.28	2269.08	-8.607	$<2 \cdot 10^{-16}$
-3dB terminal frequency ~ noiseband + animal + (1 | date/event)				
	Mean ± s.e.m	df	t-ratio	p-value
Intercept (Control trials, bat #1)	56.98 ± 0.19	236.39	305.09	$<2 \cdot 10^{-16}$
15-30 kHz	-0.68 ± 0.25	1439.42	-2.67	$7.72 \cdot 10^{-3}$
30-45 kHz	-2.29 ± 0.27	2282.71	-8.47	$<2 \cdot 10^{-16}$
30-55 kHz	-1.28 ± 0.27	2282.97	-4.68	$3.02 \cdot 10^{-6}$
30-90 kHz	-1.51 ± 0.27	2282.96	-5.51	$3.95 \cdot 10^{-8}$
55-90 kHz	-0.87 ± 0.27	2282.54	-3.17	$1.53 \cdot 10^{-3}$
70-90 kHz	-1.84 ± 0.27	2282.24	-6.72	$2.25 \cdot 10^{-11}$
Bat #2	-0.45 ± 0.24	2270.33	-1.90	0.058
Bat #3	-1.11 ± 0.24	2266.27	-4.74	$2.22 \cdot 10^{-6}$
Bat #4	-2.01 ± 0.24	2267.72	-8.51	$<2 \cdot 10^{-16}$
Bat #5	-1.03 ± 0.24	2268.46	-4.36	$1.39 \cdot 10^{-5}$